Supporting Information

$GaPS_2Se_2$ Monolayer: Novel Stable 2D Janus Semiconductor with Anisotropic Properties for Spontaneous Water splitting under the Irradiation of Solar Light

Yuefei Zhang[a], *Xuefei Liu*[a,b*], *Zhen Wang*[a]*, *Xihao Chen*[c], *Wenjun Xiao*[a], *Tianyun Liu*[a], *Wei Gong*[d]*, *Xun Zhou*[a*], *Xianglin Pei*[d], *Zhaofu Zhang*[e]

[a]School of physics and electronic science, Guizhou Normal University, Guiyang 550025, China.
[b]Guizhou Provincial Key Laboratory of Computational Nano-Material Science, Guizhou Education University, Guiyang 550025, China.
[c] School of Materials Science and Engineering, Research Institute for New Materials and Technology, Chongqing University of Arts and Sciences, Chongqing，402160, China
[d] School of materials and architectural engineering, Guizhou Normal University, Guiyang 550025, China.
[e] The Institute of Technological Sciences, Wuhan University, Wuhan 430072, China
.

Note 1: Photocatalytic water splitting contains two half-reactions, the oxygen evolution reaction (OER) and hydrogen evolution reaction (HER), where the two half-reactions can be obtained based on the theory developed by Nørskovet *al*[1]. That is the adsorption energy difference (ΔG) in the water redox reaction, which can be calculated as:

$$\Delta G = \Delta E_{DFT} + \Delta ZPE - T\Delta S \quad (S1)$$

In which ΔE_{DFT} is the adsorption energy obtained from DFT calculation, ΔZPE is the zero-point energy, T is the temperature at 298.15 K and ΔS is the entropy difference between the adsorption state and gas phase.

The OER process is the half-reaction of the photocatalytic water splitting process, where the reaction mechanism can be divided into two parts: the acid condition and the alkaline condition. Under acid medium, the total reaction is $2H_2O \rightarrow O_2 + 4H^+ + 4e^-$, and the reaction is $4OH^- \rightarrow O_2 + H_2O + 4e^-$, As for the OER process, there are four elementary steps to transfer H_2O to O_2, which could be described as following under acid conditions:

$$* + H_2O \rightarrow *OH + H^+ + e^- \quad (S2)$$

$$*OH \rightarrow *O + H^+ + e^- \quad (S3)$$

$$*O + H_2O \rightarrow *OOH + H^+ + e^- \quad (S4)$$

$$*OOH \rightarrow * + O_2 + H^+ + e^- \quad (S5)$$

Where '*', H^+, *and* e^- are the $GaPS_2Se_2$ substrate, proton, and electron respectively. And **OH*, **O*, **OOH* are the adsorption intermediate.

The corresponding reaction pathway for OER under alkaline condition is described as follow:

$$* + OH^- \rightarrow *OH + e^- \quad (S6)$$

$$*OH + OH^- \rightarrow *O + H_2O + e^- \quad (S7)$$

$$*O + OH^- \rightarrow *OOH + e^- \quad (S8)$$

$$*OOH + OH^- \rightarrow * + O_2 + H_2O + e^- \quad (S9)$$

Meanwhile, the HER as the other reaction halfway could be summarized as two reaction mechanisms, including the Volmer–Heyrovsky and Volmer–Tafel reaction pathways, and both of them occur in two steps. Among Volmer–Heyrovsky reaction pathway, the H^+ adsorbed on the substrate, then the second H^+ from the solution reacts with first *H to form the H_2 molecule in the

Heyrovsky step under acid condition, and the corresponding reaction equations are as follows:

$$* + H^+ + e^- \rightarrow *H \quad \text{(S10)}$$

$$*H + H^+ + e^- \rightarrow H_2\,(g) \quad \text{(S11)}$$

Under alkaline solution, the typical HER can be concluded by:

$$H_2O + e^- + * \rightarrow *H + OH^- \quad \text{(S12)}$$

$$H_2O + *H + e^- \rightarrow * + H_2 + OH^- + * \quad \text{(S13)}$$

And the $*H$ is the adsorption intermediate. As for the Volmer–Tafel reaction pathways, two H+ adsorbed on the substrate's surface and form an H_2 molecule. Which can be described as follow:

$$*H + *H \rightarrow H_2 + 2* \quad \text{(S14)}$$

For each of the elementary steps, the free energy difference under the effect of PH and an extra potential bias can be written as:

$$\Delta G_1 = G_{*OH} + 1/2G_{H2} - G_* - G_{H2O} + \Delta G_U - \Delta G_{PH} \quad \text{(S15)}$$

$$\Delta G_2 = G_{*O} + 1/2G_{H2} - G_{*OH} + \Delta G_U - \Delta G_{PH} \quad \text{(S16)}$$

$$\Delta G_3 = G_{*OOH} + 1/2\,G_{H2} - G_{*O} - G_{H2O} + \Delta G_U - \Delta G_{PH} \quad \text{(S17)}$$

$$\Delta G_4 = \Delta G_* + 1/2G_{H2} - G_{*O2} - G_{*OOH} + \Delta G_U - \Delta G_{PH} \quad \text{(S18)}$$

$$\Delta G_5 = G_{*H} - 1/2\,G_{H2} - G_* + \Delta G_U + \Delta G_{PH} \quad \text{(S19)}$$

$$\Delta G_6 = \Delta G_* + 1/2G_{H2} - G_{*H} + \Delta G_U + \Delta G_{PH} \quad \text{(S20)}$$

Where $\Delta G_1, \Delta G_2, \Delta G_3,$ and ΔG_4 belong to the OER process and ΔG_5 and ΔG_6 are the HER process. And $G_{*OH}, \Delta G_U, \Delta G_{PH}, G_{*O}, G_{*OOH}, G_{O2}, G_{*H},$ and G_{H2} are the adsorption free energy of OH, O, OOH, O_2, H, and H_2. $\Delta G_U, \Delta G_{PH}$ is the extra potential bias, energy contribution to different PH concentrations, in which $\Delta G_{PH} = K_BT \times ln10 \times pH$, $\Delta G_U = -eU$. The Gibbs free energy of O2 (G_{O2}) will be obtained by $G_{O2} = G_{H2O} - 2G_{H2} + 4.92$ eV, because the DFT method fails to accurately describe the high-spin ground state of the O2 molecule.

Note 2: As depicted in **Figure.S1**, two bonding sites, namely, site 1 and site 2 are chosen for judging the bonding nature between Ga and Se, as well as P and Se atoms, respectively. For comparison, the COHP for $GaPS_4$ is also considered. Generally, the negative value of COHP under the Fermi level represents the antibonding state and vice versa. As shown in **Fig.S1**, for the same sites, two antibonding states are observed in the Ga-S bond in the $GaPS_4$ system. However, none of the antibonding states formed in the $GaPS_2Se_2$ system for Ga-Se bonds, indicating that the Ga-Se shows stronger covalent bonds than Ga-S in the $GaPS_4$ system. However, all the bonding states of P-S/Se show antibonding states in both $GaPS_4$ and $GaPS_2Se_2$ systems, demonstrating the weak covalent bonding of P-S/Se.

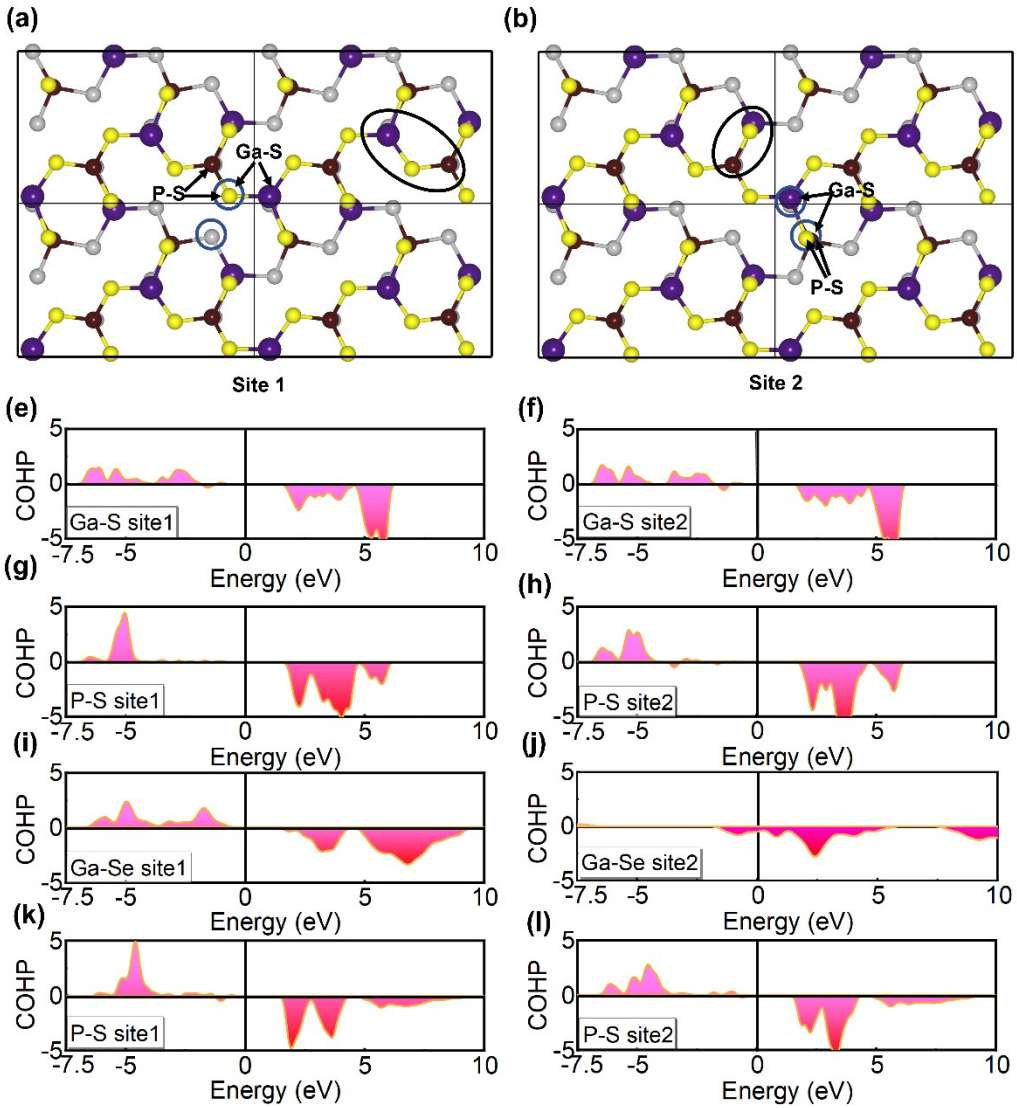

Figure S1: For the $GaPS_4$ and $GaPS_2Se_2$ system, each S/Se atom bonds with one Ga atom and one P atom (forming Ga-S-P and Ga-Se-P), respectively. As it can be seen from the geometry, the bonding nature between Ga-S-P and Ga-Se-P can be classified into two categories. The one is Ga-S-P or Ga-Se-P which is labeled by a black oval in the left figure (the two can be regarded as one site since they own similar bonding structures and they can superposition by rotating certain angles), we defined it as Site 1 (a). Similarly, the other one is also marked by a black oval (right figure), which is defined as Site 2 (b). (e)-(l) is the COHP between them, and the Fermi level is -3.44 eV in our calculation, which align at 0 eV for all of them.

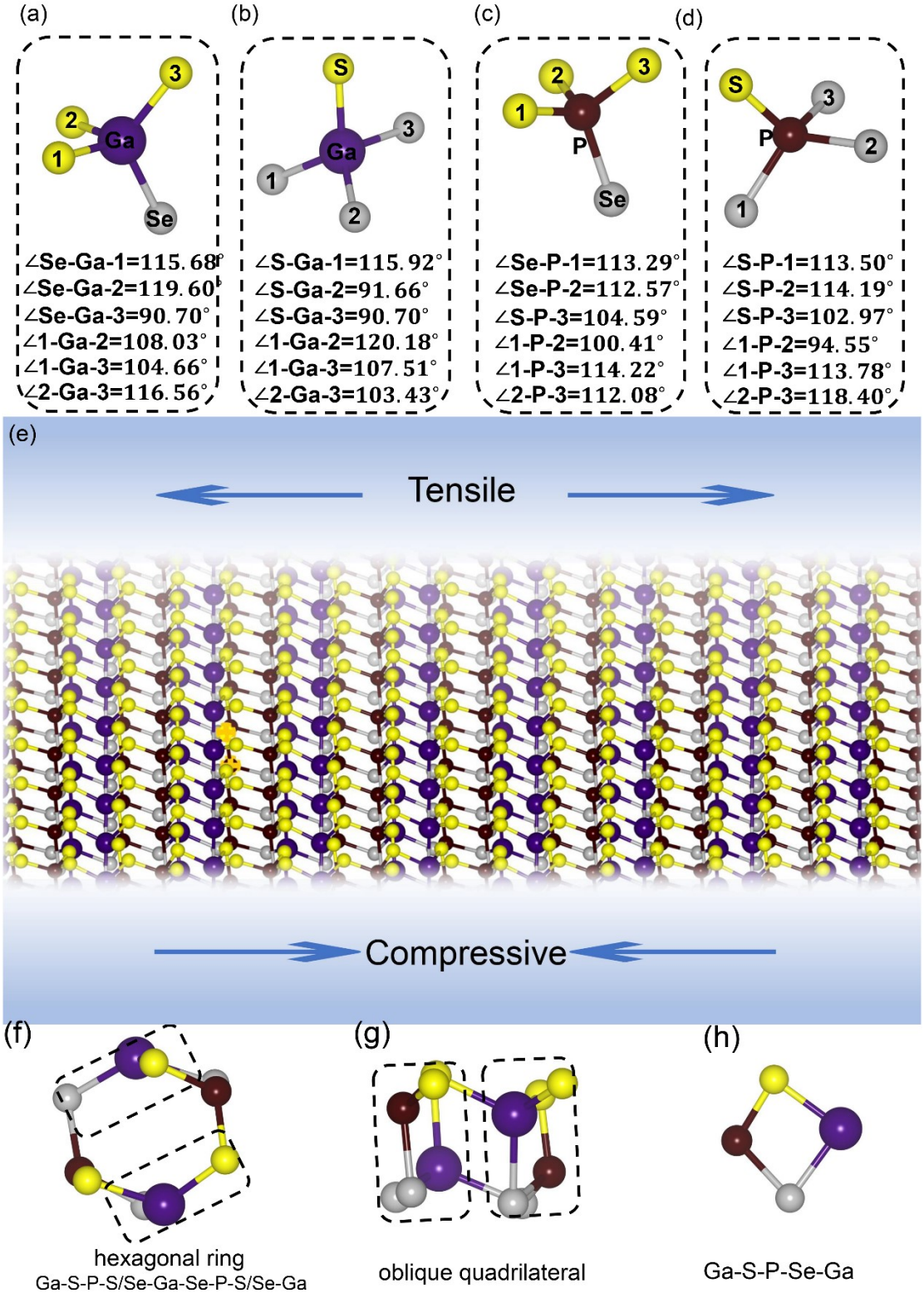

Figure S2: Atomic structure of GaS_3Se (a), $GaSSe_3$ (b), PS_3Se (c), $PSSe_3$ (d). The S and Se elements are marked with numbers, and the angles between three atoms are listed as well. (e) The hexagonal ring in the primitive-cell (e), and each of the hexagonal contains two oblique quadrilateral (f), and

the structure of oblique quadrilateral (g). (h), (i) The tensile/compression strain applied from the a and b direction of the $GaPS_2Se_2$ monolayer. and the consistency of strained.

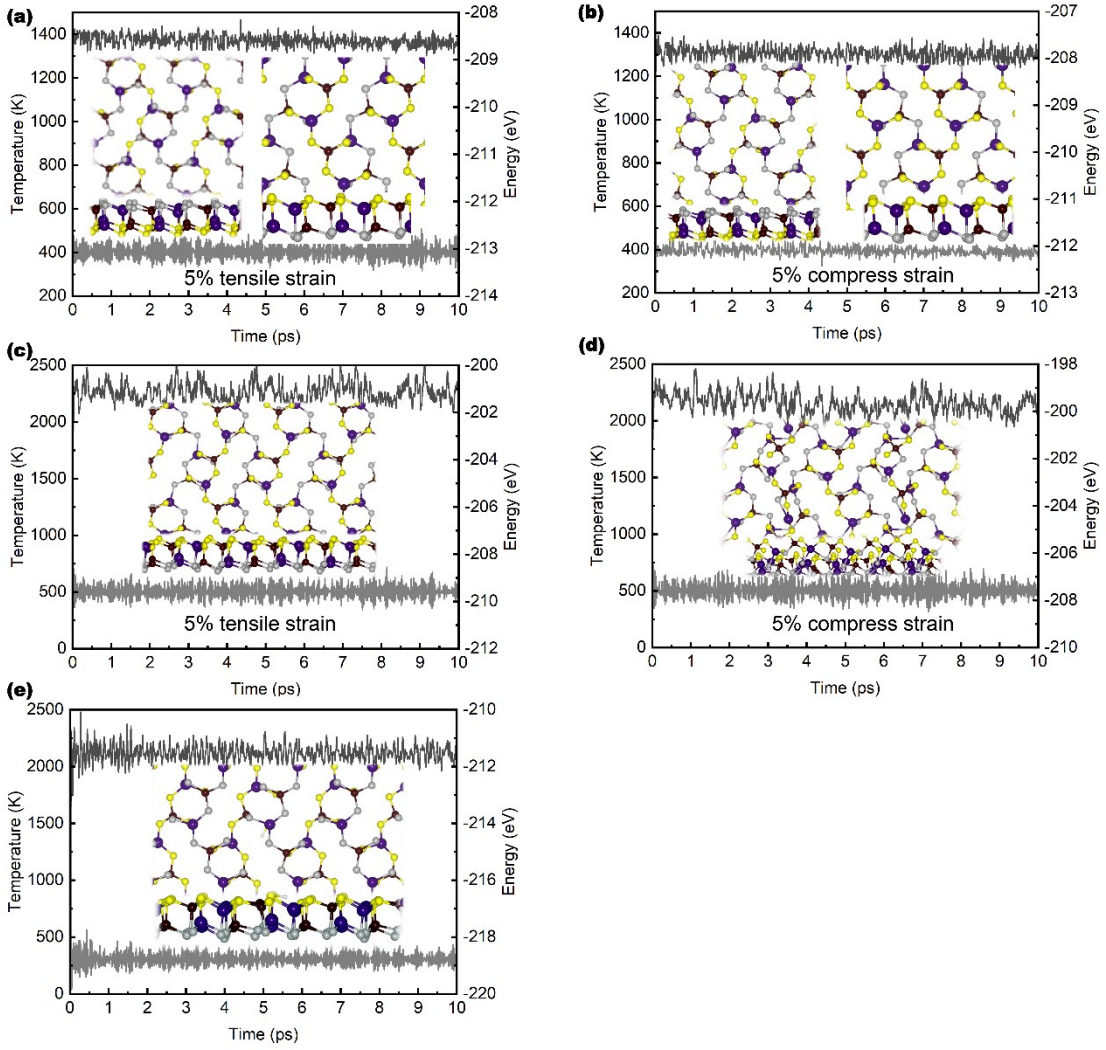

Figure S3: (a), (b) the AIMD for the applied biaxial strain (±5%) at 400K lasting for 10 ps for the 1×2×1 supercell of $GaPS_2Se_2$ monolayer, the inset pictures are the top and side structure of $GaPS_2Se_2$ after AIMD simulation and optimizing for the simulated structures (c), (d) the AIMD for the applied biaxial strain (±5%) at 500K lasting for 10 ps for the 1×2×1 supercell of $GaPS_2Se_2$ monolayer. (e) the AIMD simulation at 300K (To modulate the solvent medium, the temperature is set to 300K.) lasted for 10 ps for a 1×2×1 supercell.

Note 3: Calculation of the anisotropic Young's Modulus, Shear Modulus, and Poisson's Rate.

The ***Hook's law*** under the in-plane stress condition was implemented in this paper to explore the anisotropic properties of 2D $GaPS_2Se_2$, in which the correlation of stress (σ), elastic constant tensile (C_{ij}), and strain ε were corrected and expressed as[2]:

$$\sigma_{xx} = C_{11}\varepsilon_{xx} + C_{12}\varepsilon_{yy} \quad (S21)$$

$$\sigma_{yy} = C_{12}\varepsilon_{xx}\ C_{22}\varepsilon_{yy} \quad (S22)$$

$$\varepsilon_{zz} = 2C_{66}\varepsilon_{zz} \quad (S23)$$

where the standard Voigt notation was implemented to simplify the tensile notation. And the elastic constant can be obtained by the following equation[3]:

$$E_S = 1/2C_{11}\varepsilon_{xx}^2 + 1/2C_{22}\varepsilon_{yy}^2 + C_{12}\varepsilon_{xx}\varepsilon_{yy} + 2C_{66}\varepsilon_{zz}^2 \quad (S24)$$

Here, E_S is the strain energy, and the tensile strain can be defined as $\varepsilon = (L_i - L_{i0})/L\ (I = x, y)$, in which the L_i and L_{i0} is the strained and unstrained lattice constant along the x and y-direction with a variety from -2% to 2% and a 0.5% increment. Based on this, the orientation-dependent Young's Modulus $E(\theta)$, Shear Modulus $G(\theta)$, and Poisson's Rate $\nu(\theta)$ can be calculated as[4, 5]:

$$E^{-1} = S_{11}cos^4\theta + S_{22}sin^4\theta + 2S_{16}cos^3\theta sin\theta + 2S_{26}sin^3\theta cos\theta + (2S_{12} + S_{66})cos^2\theta sin^2\theta \quad (S18)$$

$$-\nu(\theta)/E(\theta) = A + Bcos(4\theta + \psi_1 \quad (S25)$$

in which

$$A = [(S_{11} + S_{22} - S_{66})/2 + 3S_{13}]/4 \quad (S26)$$

$$B = \frac{\sqrt{(S_{26} + S_{16})^2 + [S_{12} - (S_{11} + S_{22} - S_{66})/2]^2}}{4} \quad (S27)$$

$$\tan\psi_1 = \frac{S_{26} - S_{16}}{S_{12} - (S_{11} + S_{22} - S_{66})/2} \quad (S28)$$

$$1/4G(\theta) = C + Dcos(4\theta + \psi_2) \quad (S29)$$

Here, C, D, and ψ_1 can be obtained by:

$$C = (S_{11} + S_{22} - S_{12} + S_{66})/8 \quad (S30)$$

$$D = \frac{\sqrt{(S_{66} + 2S_{12} - S_{11} - S_{22})^2/4 + (S_{26} - S_{16})^2}}{4} \quad (S31)$$

$$\tan\psi_2 = \frac{2(S_{16} - S_{26})}{(S_{66} + 2S_{12} - S_{11} - S_{22})} \quad (S32)$$

161 Where θ belongs to [0 - 2π], and $S_{ij} = C_{ij}$.

162

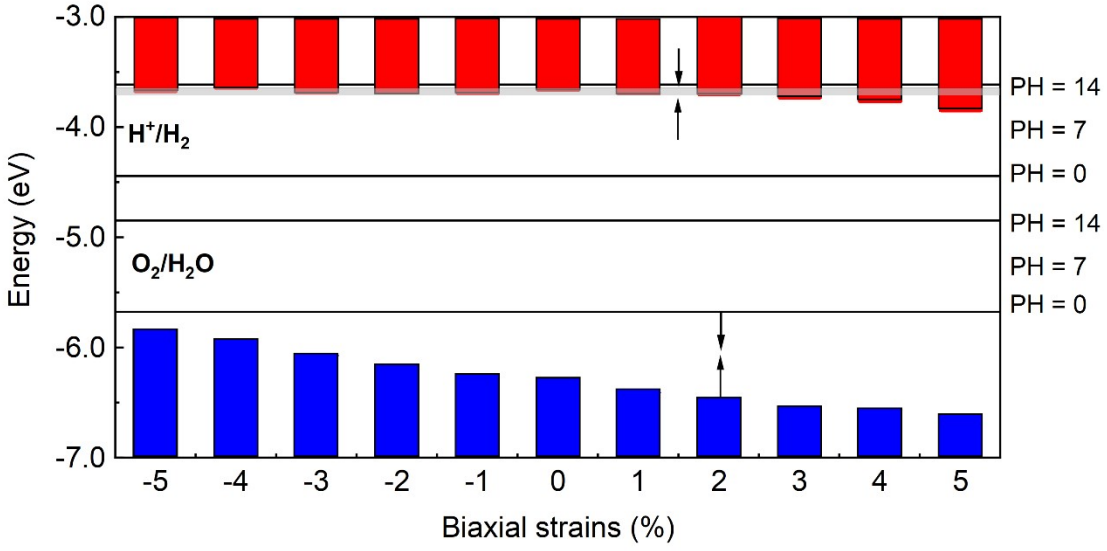

163

164 Figure S4: Strain tunable band edge positions for $GaPS_2Se_2$ monolayer under HSE functional

165 (does not consider the external electric field).

166

167 **Note 4**: Thermodynamic Oxidation and Reduction Potentials of $GaPS_2Se_2$ Monolayer in Aqueous
168 Solution

169 To shed light on the thermodynamic stability of the $GaPS_2Se_2$ monolayer in an aqueous
170 solution, the theory developed by Chen[6] was employed in this paper. The reduction of $GaPS_2Se_2$
171 monolayer by the photo-generated electron can be described by the following formula:

172 $$GaPS_2Se_2 + 7/2H_2 \rightarrow Ca + H_3P + H_2S + H_2Se \quad \text{(S33)}$$

173 Where the Gibbs free energy difference of the productions and the reactants are the thermodynamic
174 reduction potential of the $GaPS_2Se_2$ monolayer (φ^{re}), which can be calculated by:

175 $$\varphi^{re} = -[\Delta_fG^0(Ga) + \Delta_fG^0(H_3P) + \Delta_fG^0(H_2S) + \Delta_fG^0(H_2Se) - \Delta_fG^0(GaPS_2Se_2) - 7/2\Delta_fG^0(H_2)]/7eF +$$

176 $$\phi(H^+/H_2) \quad \text{(S34)}$$

177 in which $\Delta_fG^0(Ga)$, $\Delta_fG^0(H_3P)$, $\Delta_fG^0(H_2S)$, $\Delta_fG^0(H_2Se)$, $\Delta_fG^0(GaPS_2Se_2)$, $\Delta_fG^0(H_2)$ are the Gibbs free
178 energy formation of Ga, H_3P, H_2S, H_2Se, and $GaPS_2Se_2$, H_2, respectively, e is the electronic charge,
179 F is the Faradic constant. Among them, the $\Delta_fG^0(Ga)$, $\Delta_fG^0(H_3P)$, $\Delta_fG^0(H_2S)$, $\Delta_fG^0(H_2Se)$ could be
180 found in the CRC Handbook of Chemistry and Physics[7], which was concluded in table S1.
181 Meantime, the Gibbs free energy formation of the $GaPS_2Se_2$ ($\Delta_fG^0(GaPS_2Se_2)$) is approximated to
182 the formation energy of $GaPS_2Se_2$, which was defined by:

$$E_{form} = E_{GaPS2Se2} - 4E_{Ga} - 4\,E_P - 8E_S - 8E_{Se} \quad \text{(S35)}$$

here, $E_{GaPS2Se2}$ could be obtained by DFT calculation, and E_{Ga}, E_P, E_S, E_{Se} is the chemical potential under the most stable state, which is -3.03 eV, -5.41 eV, -4.14 eV, and -3.50 eV, respectively. According to our DFT result, the energy value of the $GaPS_2Se_2$ unit is -105.06 eV, thus the formation energy of $GaPS_2Se_2$ is -0.43 eV per atom eventually according to the above equation. Finally, the ϕ^{re} was calculated as -0.04 V (*vs CHE*).

The $GaPS_2Se_2$ monolayer could be oxidized by the photogenerated holes according to the following equation.

$$2GaPS_2Se_2 + 3H_2O \rightarrow Ga_2O_3 + 2P + 4S + 4Se + 3H_2 \quad \text{(S36)}$$

similarly, the thermodynamic oxidation potential of the $GaPS_2Se_2$ monolayer (ϕ^{re}), which could be defined as follows:

$$\phi^{ox} = [\Delta_fG^0(P) + \Delta_fG^0(Se) + \Delta_fG^0(S) + \Delta_fG^0(Ga_2O_3) - \Delta_fG^0(GaPS_2Se_2) - 3\Delta_fG^0(H_2O)]/6eF + \phi(H^+/H_2) \quad \text{(S37)}$$

in which $\Delta_fG^0(P)$, $\Delta_fG^0(Se)$, $\Delta_fG^0(S)$, $\Delta_fG^0(Ga_2O_3)$ are the standard Gibbs free energy of formation of P, Se, S, and Ga_2O_3, which is also found in the CRC Handbook of Chemistry and Physics. By implementing the equations above, the calculated value of ϕ^{ox} is 3.56 V (*vs NHE*), which was plotted in Figure 8.

Table S1, the Gibbs free energy of each species used in this paper

Molecular Formula	Δ_fG^0	**Molecular Formula**	Δ_fG^0
Ga	233.7	H_2S	-33.4
P	280.1	H_3P	13.5
S	187.0	H_2Se	15.9
Se	236.7	Ga_2O_3	-998.3
H_2O	-237.1	H_2	0

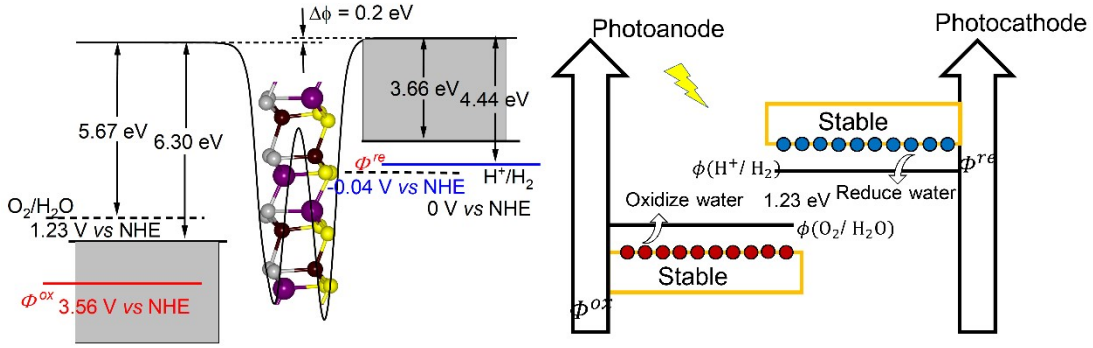

Figure S5 redox potential of $GaPS_2Se_2$ and position of CBM and VBM after aligning with the reduction/oxidation potential of water.

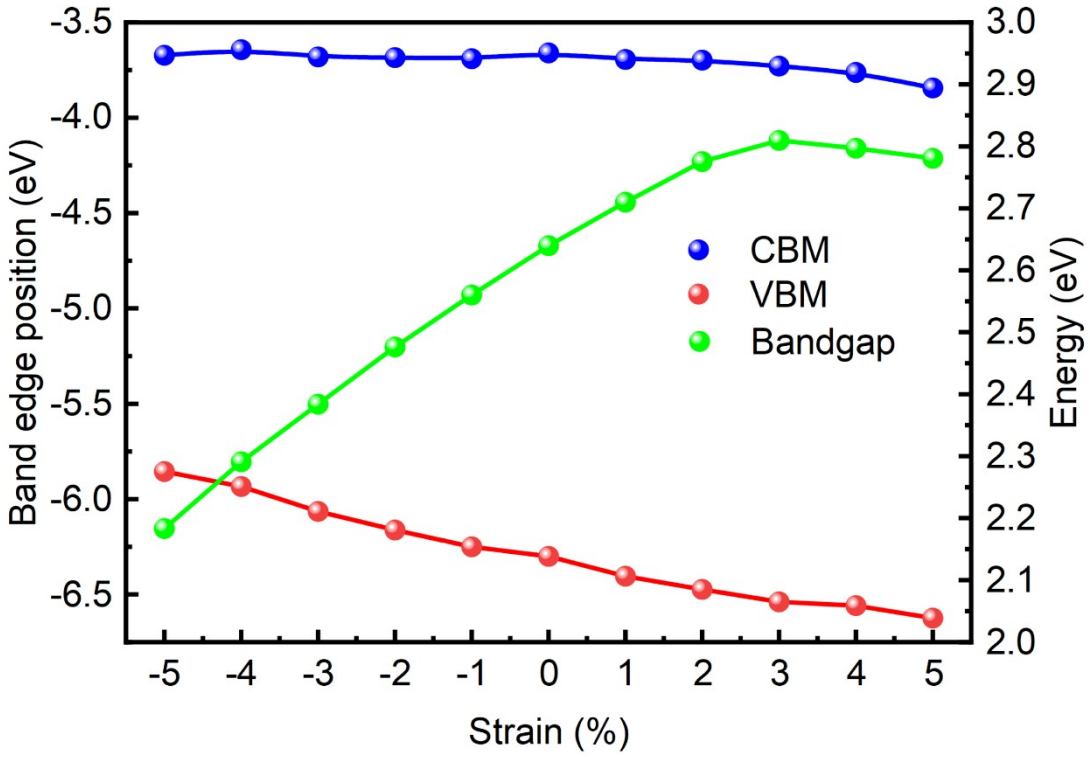

Figure S6: Variations of CBM, VBM, and bandgap of $GaPS_2Se_2$ monolayers with biaxial and uniaxial lattice strains from -5% (compression) to 5% (tension).

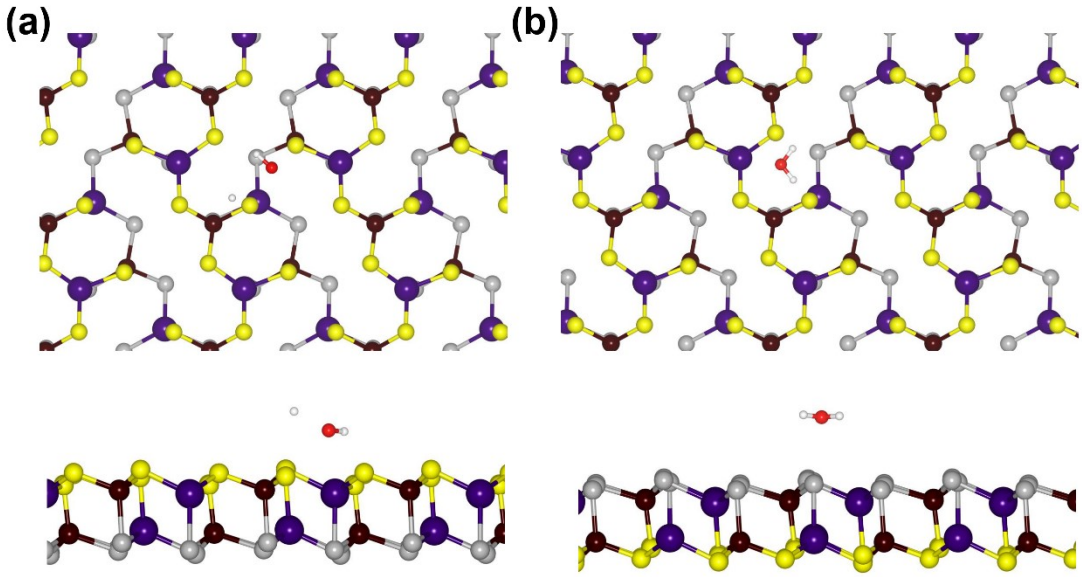

Figure S7: Top and side views of the adsorption structures of H_2O molecule on the S (a) and Se (b) sides.

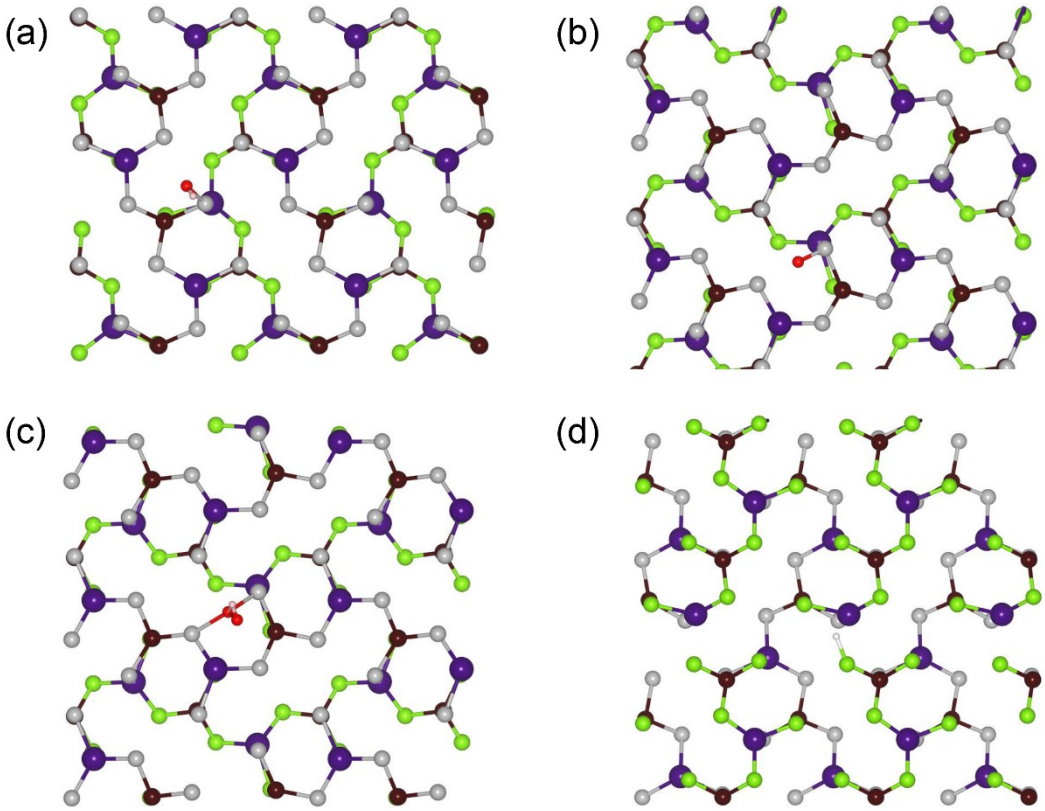

Figure S8: Structures of the adsorbed species (OH, O, OOH, H) of the applied 2% tensile strain system.

[1] K.S. Novoselov, A.K. Geim, S.V. Morozov, D. Jiang, Y. Zhang, S.V. Dubonos, I.V. Grigorieva, A.A. Firsov, Electric field effect in atomically thin carbon films, Science, 306 (2004) 666-669.

[2] V. Wang, W.T. Geng, Lattice Defects and the Mechanical Anisotropy of Borophene, J. Phys. Chem. C, 121 (2017) 10224-10232.

[3] R.C. Andrew, R.E. Mapasha, A.M. Ukpong, N. Chetty, Mechanical properties of graphene and boronitrene, Phys. Rev. B, 85 (2012) 1-9.

[4] S.D. Baranovskii, Theoretical description of charge transport in disordered organic semiconductors, Phys. Status Solidi B, 251 (2014) 487-525.

[5] C. Jasiukiewicz, T. Paszkiewicz, S. Wolski, Auxetic properties and anisotropy of elastic material constants of 2D crystalline media, Phys. Status Solidi B, 247 (2010) 1247-1247.

[6] S. Chen, L.-W. Wang, Thermodynamic Oxidation and Reduction Potentials of Photocatalytic Semiconductors in Aqueous Solution, Chem. Mater., 24 (2012) 3659-3666.

[7] G. Baysinger, Berger, L. I., Goldberg, R. N., Kehiaian, H. V., & Kuchitsu, K., CRC handbook of chemistry and physics. , (2015) National Institute of Standards and Technology.